Effects of Crosslink Density on Mechanical Properties of High Glass Transition Temperature Polycyanurate Networks

OLIVIER GEORJON,* JOCELYNE GALY

Laboratoire des Matériaux Macromoléculaires, INSA-UMR 5627, 69621 Villeurbanne cedex, France

Received 19 July 1996; accepted 19 December 1996

ABSTRACT: Polycyanurate networks of different architecture were synthesized using different curing cycles. Networks with a variable extent of reaction were obtained; the small variation of the cyanate conversion (0.8 to 1) corresponds to a large variation of glass transition temperature (150–290°C) and crosslink density. The mechanical behavior at small and large deformations and the fracture toughness were examined at room temperature and related to the network structural parameters. To explain the puzzling variation of the yield stress and yield strain with the cyanate conversion, recovery experiments were conducted to discriminate anelastic deformation from plastic deformation. © 1997 John Wiley & Sons, Inc. J Appl Polym Sci **65:** 2471–2479, 1997

Key words: cyanate; crosslink density; mechanical properties; deformation recovery

INTRODUCTION

The development of new high performance polymers over the last decade was stimulated primarily by the demands of the aerospace and electronics industries for high glass transition temperature (T_g) materials with low dielectric losses. Epoxy resins are so far the most widely used thermosets for structural composites, but their poor hot and wet performances limit the applications in which they may be used. In such circumstances, higher temperature performance resins are needed and cyanate ester resins are among the candidates to fulfill this role.

Bifunctional cyanate ester monomers homopolymerize through a cyclotrimerization reaction to form 3-dimensional networks as depicted in Figure 1. These networks are termed polycyanurates. The cure chemistry[1–5] as well as the network buildup[6–8] of cyanate esters has been reported in several useful articles. However, much less interest has been paid to relationships between molecular architecture and macroscopic physical properties of polycyanurates.[9,10] Fully cured materials are quite ideal networks in which all linkages between crosslinks are identical. Owing to the high crosslink density and aromaticity of the polymer, very high glass transition temperatures are expected, typically in the 290–300°C range. This major advantage as compared to conventional epoxies is obtained only with a postcure cycle at high temperature. If such a condition is not achieved, an uncomplete reaction will result in a significant amount of network defects (i.e., chain extension and dangling chains) that in turn will dramatically affect the material properties.

Our strategy was to synthetize polycyanurate networks with different crosslink densities by stopping the polymerization at different extents of reaction. A statistical approach provided a theoretical relationship between the cyanate conversion (i.e., the amount of reacted functions) and the relevant postgel quantities (gel and sol fractions, crosslink density). Then a previous study

Correspondence to: Dr. J. Galy.
* *Present address:* Exxon Chemical Europe Inc., Hermeslaan 2, 1831 Machelen, Belgium.

Journal of Applied Polymer Science, Vol. 65, 2471–2479 (1997)
 CCC 0021-8995/97/122471-09

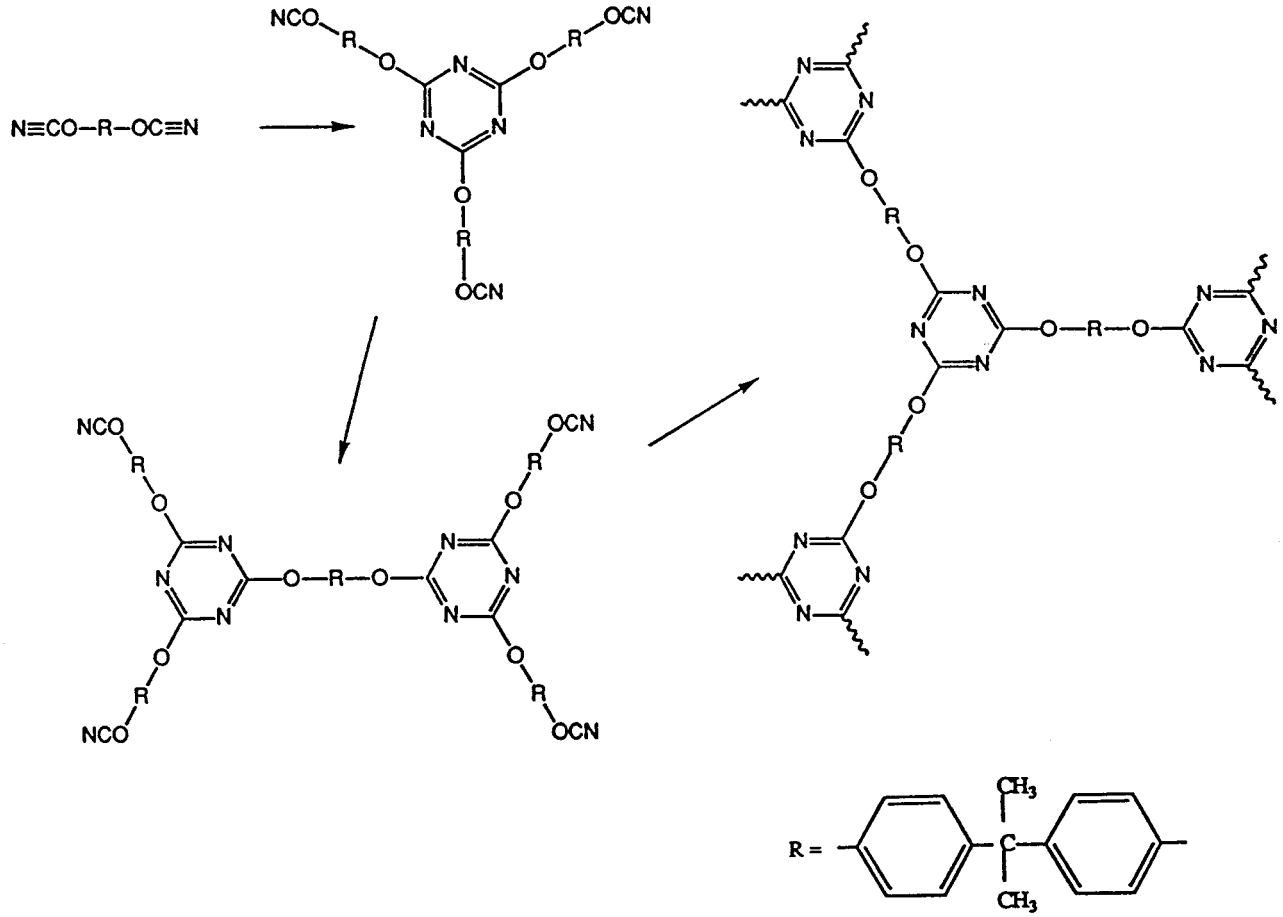

Figure 1 Monomer structure and network formation.

reported the effect of cyanate conversion on volumetric properties.[11] Focusing on the latest stages of cure, we demonstrated that the formation of bulky triazine crosslinks induces a steric hindrance that reduces the network ability to pack effectively upon cooling, thus creating an increasing fraction of unoccupied volume holes on a nanometer scale. This phenomenon was assessed by positron annihilation lifetime spectroscopy and shed some light on the evolution of different material properties of practical interest, that is, a decrease in density and an increase in moisture absorption as the extent of conversion increases. Keeping this in mind, we address the relation between cyanate conversion and mechanical properties with successive emphasis on small strain, large strain, and fracture properties. A future article will focus on viscoelastic behavior in the glassy state, with a detailed assignment of the secondary relaxations in terms of molecular motions.[12]

EXPERIMENTAL

Materials

The cyanate ester monomer used in this work was the dicyanate of bisphenol A supplied by Ciba–Geigy (commercial name Arocy B10) as a high purity (>99.5%) crystalline powder. It was cured either with a typical catalytic system consisting of 200 ppm of Cu^{++} (copper acetyl acetonate) dissolved in 200 phr nonylphenol or without a catalyst. Sample preparation and curing cycles were similar to those previously reported.[11] Based on the results of an isothermal kinetic study, they were selected to reach cyanate conversions, x, ranging from 80 to 100%. Four uncatalyzed (100, 95, 90, and 85) and three catalyzed (C100, C91, and C82) polycyanurate networks were synthesized. Main characteristics such as cyanate conversion measured by differential scanning calorimetry or infrared spectroscopy, glass transition, and theoret-

Table I Main Characteristics of Polycyanurate Networks

Network	100	95	90	85	C100	C91	C82
T_g (°C)	290	265	212	168	275	202	149
x (DSC)	1	0.96	0.91	0.85	1	0.91	0.82
X (mol/kg)	2.39	1.94	1.52	1.14	2.34	1.57	0.91
ρ	1.207	1.212	1.219	1.225	1.202	1.215	1.225

Glass transition temperature, T_g, and cyanate conversion, x, measured by DSC. Theoretical crosslink density X. Density ρ.

ical crosslink density are summarized in Table I. There is a unique one to one relationship between T_g and conversion and it is important to note that very different polymer architectures were obtained (variations in T_g of more than 140°C and differences of more than 100% in crosslink density), in spite of the apparently narrow range of conversion.

Techniques

All mechanical tests were run at room temperature.

Small Deformations

Stiffness behavior at small deformations were investigated by two different methods. Uniaxial tensile Young's moduli, E, were determined at a low strain rate of $1.66\ 10^{-4}\ s^{-1}$ using rectangular bars of $100 \times 15 \times 6\ mm^3$. The deformation measurement was accurately monitored using strain gages from Vishay micromeasures. In addition, ultrasonic wave velocity measurements were used to access the material behavior at extremely high strain rates. Sound velocities in the longitudinal (V_L) and in the transversal mode (V_T) were determined at a frequency of 5 MHz from the time of flights of pulsed signals between parallel free surfaces of thick samples (6 mm). Then the ultrasonic shear (G_u), Young's (E_u), and bulk compressibility (B_u) moduli, as well as the Poisson's ratio (ν) were computed according to the following expression:

$$G_u = \rho V_T^2$$

$$E_u = \rho V_T^2 \frac{3V_L^2 - 4V_T^2}{V_L^2 - V_T^2}$$

$$\nu = \frac{1}{2}\frac{V_L^2 - 2V_T^2}{V_L^2 - V_T^2}$$

$$B_u = \frac{E}{3(1 - 2\nu)}$$

Large Deformations

Rectangular samples ($15 \times 15 \times 6\ mm^3$) were tested in uniaxial compression mode at a strain rate of $1.11\ 10^{-3}\ s^{-1}$ to give the yield stress at the plateau, σ_p, and the corresponding strain ε_p, before the onset of strain hardening (or ε_y and σ_y at the maximum).

Fracture Toughness

The concept of the linear elastic fracture mechanism was employed. The stress intensity factor, K_{IC}, was determined using a 3-point bending test on single-edge notched (SEN) samples. The displacement rate was 1 mm min^{-1}.

RESULTS AND DISCUSSION

Small Deformations

The variation of the Young's modulus of the polycyanurate networks with the cyanate conversion is shown in Figure 2. The Young's modulus de-

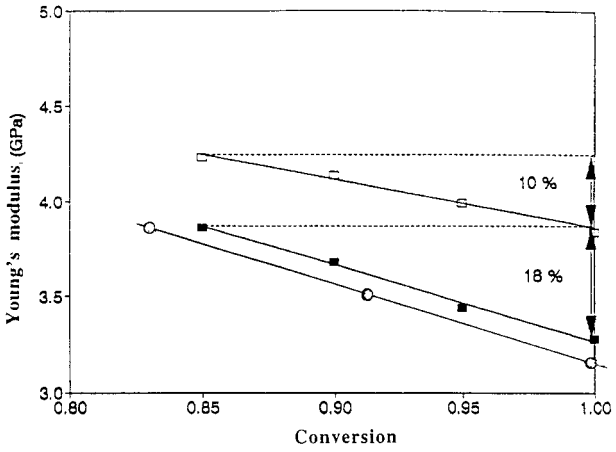

Figure 2 Variation of the (■) Young's modulus and (□) ultrasonic modulus as a function of conversion (uncatalyzed networks). (○) Variation of the Young's modulus of catalyzed networks.

creased as the conversion increased and when a catalyst was used. The same trend was observed on diglycidyl ether of bisphenol A/diamine networks as the crosslink density was varied either by changing the stoichiometric ratio,[13,14] by adding a chain extender, or changing the curing cycle as in our case.[15]

Two phenomena contributed to the elasticity in the glassy state: molecular motions and cohesion of the material.

At room temperature the Young's modulus measured by a tensile test was a relaxed modulus because it is dependent upon the molecular motions that occurred. In polycyanurate networks, two sub-T_g relaxations β and γ are activated at room temperature; using dynamic mechanical spectroscopy, the β relaxation is evidenced near 0°C and the γ relaxation at −100°C, at a frequency measurement equal to 1 Hz (Fig. 3). Each relaxation is linked to a decrease of the modulus. The drop in the elastic modulus is proportional to the height of the loss peak and the temperature range over which the drop takes place is determined by the width of the loss peak. As observed on Figure 3, the magnitude of the secondary relaxations increases with the cyanate conversion. Therefore, for one part the decrease of the Young's modulus can be explained by the effect of the sub-T_g relaxations. One way to eliminate their influence is to measure the velocity of ultrasonic waves in the material. At room temperature and at a frequency of 5 MHz, β and γ relaxations are shifted to higher temperatures. Indeed β and γ relaxations follow an Arrhenius dependence with temperature and the activation energies are equal to 42 and 72 kJ/mol, respectively, for fully cured networks. According to these values, the temperatures of β and γ relaxation peaks at 5 MHz are higher than 70°C for all networks. The results obtained through ultrasonic wave propagation are reported for uncatalyzed networks in Table II. Increasing the crosslink density has the same effect on the different moduli: E_u, G_u, and B_u decrease. E_u is then compared to the Young's modulus measured by tension in Figure 2. Similar variations are observed in both cases, except that the decrease of the Young's modulus is less pronounced in the ultrasonic measurements ($\Delta E/E = 10$ vs. 18% for tensile measurements). The difference between these two values represents the effects of the molecular motions that are visualized by the secondary β and γ relaxations.

The ultrasonic modulus can be related to the cohesive energy density, E_{coh}.[12] This energy can be calculated using the method of group contributions and the data given by Fedor.[13] The cohesive energy of a partially cured polycyanurate network can be expressed as

$$E_{coh}(x) = E_{coh}\left(-O-\langle\rangle-\overset{CH_3}{\underset{CH_3}{C}}-\langle\rangle-O-\right) + 2\cdot x\cdot E_{coh}\left(-C\begin{matrix}=N-\\ \diagdown\end{matrix}\right) + 2\cdot(1-x)E_{coh}(-C\equiv N)$$

The cohesive energy is equal to 81.4 kJ/mol for a BA unit (without H), and the elementary contribution of a cyanate function $-C\equiv N$ and a $\begin{matrix}\diagdown\\ C=N-\\ \diagup\end{matrix}$ group in a triazine ring are 25.5 and 16 kJ/mol, respectively. Therefore, it becomes clear that the cohesive energy decreases with an increasing conversion. The relation between both parameters is

$$E_{coh} = 132.4 - 19x$$

The cohesive energy density is expressed by

$$\frac{E_{coh}}{V} = \frac{E_{coh} * \rho}{M_0}$$

where ρ is the density and M_0 the molecular weight of the monomer. The results are reported in Table III. They show that a good correlation is observed between the cohesive energy density and the compressibility modulus B_u. Moreover, an excellent agreement is evidenced between our series of cyanate networks and various series of epoxy/amine networks[17] (Fig. 4). In all cases an increase in the cohesive energy density leads to an increase of the compressiblity modulus, with a proportionality constant of about 10.

Finally, we have shown that the variations of the Young's modulus measured by a tensile test at 25°C as a function of cyanate conversion is explained by the surimposition of two phenomena:

1. molecular mobility in the glassy state: the relaxed modulus is linked to molecular

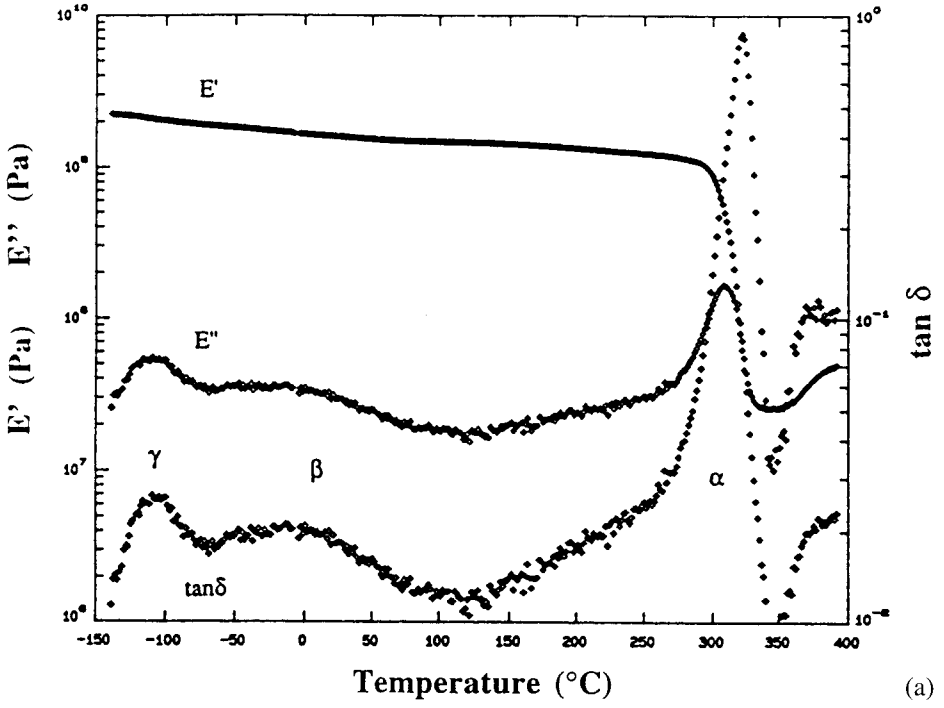

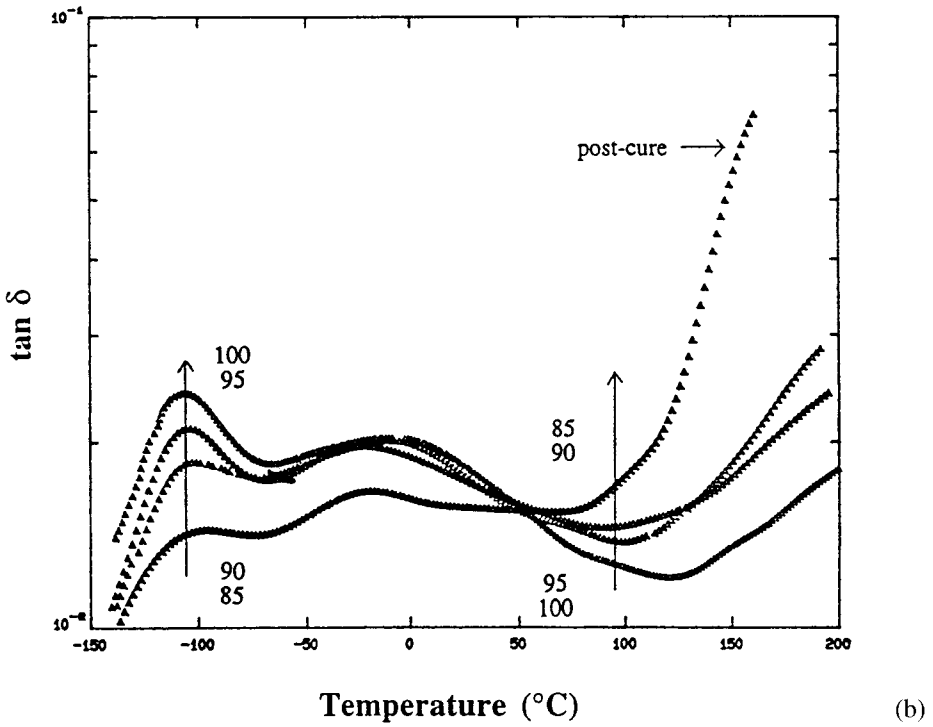

Figure 3 Dynamic mechanical spectroscopy: (a) Variation of E', E'', and tan δ as a function of temperature for a fully cured polycyanurate (x = 100%); and (b) tan δ versus temperature as a function of cyanate conversion.

Table II Characteristics Obtained Using Ultrasonic Wave Propagation on Uncatalyzed Networks

Network	V_L (m/s)	V_T (m/s)	G_u (GPa)	E_u (GPa)	B_u (GPa)	ν
100	2321	1081	1.41	3.84	4.57	0.36
95	2378	1098	1.46	3.99	4.75	0.36
90	2381	1118	1.52	4.14	4.93	0.36
85	2453	1124	1.55	4.23	5.42	0.37

motions that become more important in higher crosslinked networks; and

2. cohesion: due to the remaining —O—C≡N functions, the less crosslinked networks show a higher cohesive energy density.

Large Deformations

During a tensile test, large deformations cannot be reached because a brittle failure occurred. On the contrary, large deformations can be studied through a uniaxial compressive test. In this case cyanate networks show a high ductility. The yield characteristics are reported in Figure 5 and an unexpected variation can be noticed: the deformation ε_y (or ε_p at the plateau) increases and the yield strain σ_y (σ_p at the plateau) decreases as the crosslink density (or the conversion) is increased. Such a result is puzzling to explain in terms of plasticity because it would mean that the most rigid high T_g networks display the higher ability to undergo permanent flow. Moreover, the slope of the curve would be more pronounced if the experiments are done at a constant value of T/T_g. To perform this experiment the test temperature T needs to be increased with the network conversion and obviously the yield stress would then exhibit a decrease. This surprising result led us to a deeper investigation of the process of network deformation. It is usual to consider three components of the deformation of a polymer: elastic, anelastic and plastic deformation. When the sample is unloaded the elastic strain recovers instantaneously, the anelastic strain recovers with time, and the plastic strain is permanent. However, it has been observed that plastic deformation (ε_{pl}) can recover in a reasonable time if the polymer is heated at or above its T_g.[18,19] Therefore, we decided to study the recovery of deformation in order to differentiate anelastic (ε_{an}) from plastic deformation.

Samples are compressed until the beginning of the work hardening region. At this step the deformation is called ε_{def} (pure elastic deformation has been substracted). Then the recovery of deformation is followed in two different ways:

1. at the test temperature: the permanent or residual deformation, ε_{irr}, is measured after unloading the sample and waiting near 30 min; or
2. on heating from test temperature to T_g with a step of 10°C: between each step the sample is cooled (to avoid the effect of the

Table III Cohesive Energy Density and Compressibility Modulus as Function of Conversion for Uncatalyzed Networks

Network	E_{coh}/V (GPa)	B_u (GPa)
100	0.492	4.57
95	0.499	4.75
90	0.506	4.93
85	0.512	5.42

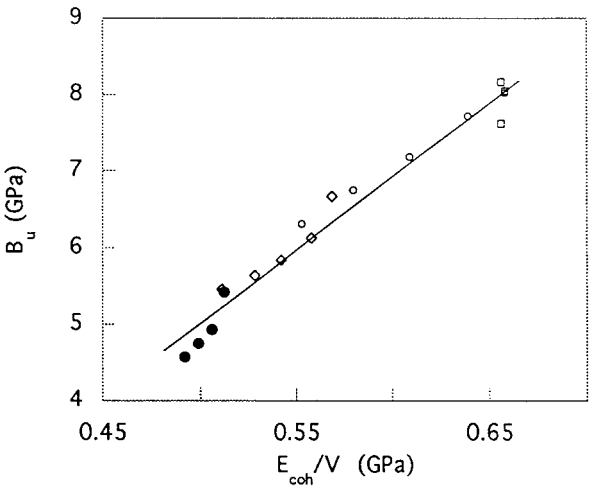

Figure 4 Variation of the compressibility modulus versus cohesive energy density: (●) cyanate networks with a conversion between 0.85 and 100% and (○, □) epoxy networks.[17]

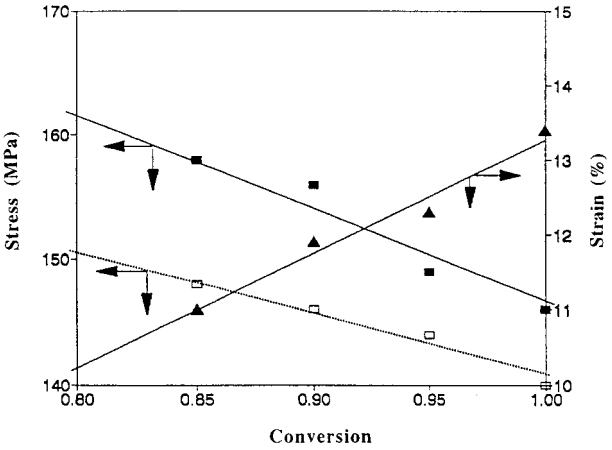

Figure 5 Variation of (■) σ_y, (□) σ_p, and (▲) ε_y versus conversion x.

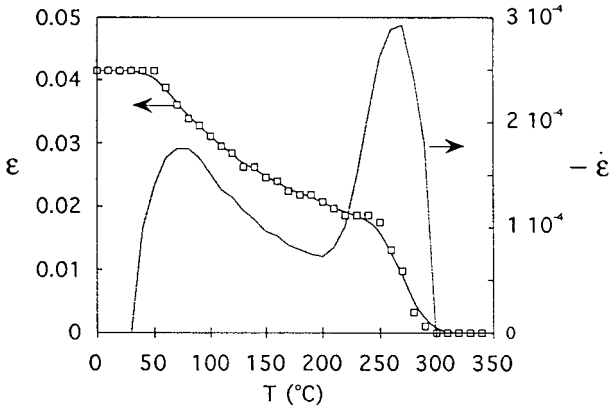

Figure 6 Deformation recovery curve of a deformed polycyanurate network (x = 100%).

thermal dilatation) and the residual deformation is measured.

A typical recovery curve and its derivative are plotted Figure 6 for the fully cured network. Two stages of deformation recovery are observed: the first one below T_g leads to the recovery of about 90% of the initial deformation and proves the overwhelming effect of anelasticity upon plasticity; the second stage appears near T_g and it is faster and a full recovery is reached.

A similar curve cannot be obtained on partially cured networks because the samples undergo further reaction as the temperature reaches the glass transition. There is a competitive mechanism between the recovery and the crosslink reaction. So we can only compare the network behavior in the glassy state between room temperature and 0.9 T_g, the temperature at which the postcured reaction may begin.

The results of the experiments conducted on the various polycyanurate networks are reported Table IV. They show the following trends:

1. whatever the network, the major part of the deformation is anelastic, even for deformation reaching the work hardening region, so it is largely after ε_y;
2. the main part of the nonelastic deformation is recovered at the test temperature (room temperature in our case); and
3. the contribution of the anelastic deformation increases as the conversion rises (i.e., the permanent deformation after unloading ε_{irr} is the lowest for the fully cured network).

The anelastic deformation processes of amorphous polymers have been described by several authors.[18–21] They suggest that deformation appears in preexisting defects, called quasipoint defects by Perez.[20] These defects are associated with local fluctuation of density. Under an application of stress, molecular motions are preferentially induced inside these defects and a localized zone of deformation called shear microdomains (SMDs) is created. The origin of ε_{an} is linked to the appearance of SMDs. Elastic energy is stored at the border of SMD; this energy can annihilate to give a plastic zone of deformation if the SMDs interact with one another. In polycyanurate networks the

Table IV Recovery of Deformation for Different Uncatalyzed Networks

Network	ε_{def} (%)	ε_{irr} (%)	$\frac{\varepsilon_{def} - \varepsilon_{irr}}{\varepsilon_{def}}$	$\varepsilon_{0.9T_g}$ (%)	$\frac{\varepsilon_{def} - \varepsilon_{0.9T_g}}{\varepsilon_{def}}$
100	16.7	4.15	0.75	1.86	0.89
95	17.0	5.46	0.68	3.05	0.82
90	15.8	6.49	0.59	3.93	0.75
85	16.3	8.31	0.49	5.65	0.65

Table V Values of Stress Intensity Factor K_{IC} and Fracture Toughness G_{IC} for Different Polycyanurate Networks

Network	K_{IC} (MPa $\sqrt{m}$)	G_{IC} (J/m^2)
100	0.8	170
95	0.5	60
90	0.5	55
85	0.3	20
C100	0.9	220
C91	0.6	90
C82	0.4	35

nature of the defects involved in the SMDs are the free volume holes (negative density fluctuation). As a matter of fact, in a previous article[11] we reported that positron annihilation lifetime spectroscopy leads to the conclusion that the free volume hole increases with an increase of conversion because the bulky triazine crosslinks disturb the packing of macromolecules. The SMD concentration is therefore the highest for the most crosslinked network.

Now the variation of σ_y and ε_y with the cyanate conversion is clear because we took into account the anelastic deformation and the concept of SMDs.

Fracture Behavior

Table V shows the results of linear elastic fracture mechanics. The values obtained for fully cured networks are very good and quite unusual for such high T_g networks. They are equivalent to those found on classical epoxy/amine networks that exhibit lower T_g of about 100°C. However, partially cured networks are very brittle: K_{IC} and G_{IC} decrease very rapidly as the conversion decreases. Figure 7 illustrates the relationship between K_{IC} and σ_p for catalyzed and noncatalyzed networks. A linear relationship is observed: a decrease in fracture toughness is related to an increased yield stress. During the test, the yield behavior at the crack tip is the main factor governing the deformation, regardless of whether this deformation can be recovered or not. The values of K_{IC} depend only of the ability of the material to undergo large deformations.

CONCLUSION

In this work the relationships between cyanate conversion (or crosslink density) and mechanical properties in a series of polycyanurate networks were investigated.

The decrease of the Young's modulus with an increase in conversion was explained by two effects: first, the cohesive energy density was lower in the more crosslinked networks; second, the magnitude of the sub-T_g relaxations, which were linked to localized molecular motions, were higher in the network of high crosslink density.

The compression tests revealed an unexpected variation of the yield stress and yield strain: as the cyanate conversion was increased, a decrease of the yield stress was observed. This result was

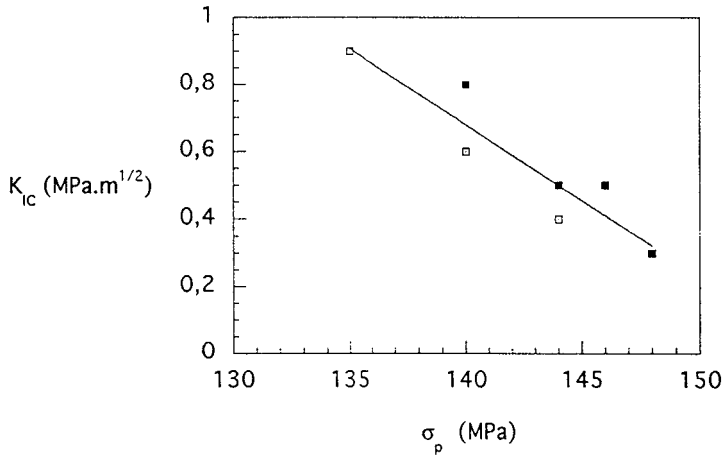

Figure 7 Variation of K_{IC} versus σ_p for (□) catalyzed networks and (■) uncatalyzed networks.

not explainable in term of plasticity (i.e., permanent deformation) and therefore led us to study the recovery of deformation upon heating. The deformation recovery was the highest for the most crosslinked networks. In such a material, the formation of shear defects during the sample loading was favored by a higher free volume fraction but these defects easily disappeared during heating. Thus, the variation of σ_y and ε_y with conversion was explained by the fact that the main contribution of the macroscopic deformation was anelasticity.

Finally, it was verified that the fracture toughness K_{IC} was controlled by the ability of the material to undergo large deformation; therefore, the highest value of K_{IC} was found for the fully cured network that exhibited the lowest value of yield stress.

The authors thank CNRS (Centre National de la Recherche Scientifique), DRET (Direction de la Recherche et des Etudes Techniques), and Aerospatiale for financial support and Pr. J. Perez and Pr. H. Sautereau for helpful discussions.

REFERENCES

1. M. Bauer, J. Bauer, and G. Kuhn, *Acta Polym.,* **37,** 715 (1986).
2. S. L. Simon and J. K. Gillham, *J. Appl. Polym. Sci.,* **47,** 461 (1993).
3. M. Bauer and J. Bauer, in *Chemistry and Technology of Cyanate Ester Resins,* Hamerton, Ed., Chapman & Hall, London, 1994, p. 15.
4. A. Osei Owuzu, G. C. Martin, and J. T. Gotro, *Polym. Eng. Sci.,* **13,** 1604 (1991).
5. O. Georjon, J. Galy, and J. P. Pascault, *J. Appl. Polym. Sci.,* **49,** 1441 (1993).
6. J. Bauer and M. Bauer, *Acta Polym.,* **38,** 16 (1987).
7. H. Stutz and P. Simak, *Makromol. Chem.,* **194,** 3031 (1993).
8. A. M. Gupta and C. W. Macosko, *Macromolecules,* **26,** 2455 (1993).
9. S. L. Simon and J. K. Gillham, *J. Appl. Polym. Sci.,* **5,** 1741 (1994).
10. D. A. Shimp and J. E. Wentworth, SAMPE, Los Angeles, 293, 1992.
11. O. Georjon and J. Galy, *Polymer,* to appear.
12. O. Georjon, J. Galy, J. F. Gerard, G. Schwach, M. Albrand, and R. Dolmazon, *Polym. Eng. Sci.* to appear.
13. Y. G. Won, J. Galy, J. F. Gerard, J. P. Pascault, V. Bellenger, and J. Verdu, *Polymer,* **31,** 1787 (1990).
14. J. Galy, J. F. Gerard, H. Sautereau, R. Frassine, and A. Pavan, *Polym. Networks Blends,* **4,** 105 (1994).
15. C. Jordan, J. Galy, and J. P. Pascault, *J. Appl. Polym. Sci.,* **46,** 589 (1992).
16. A. F. M. Barton, in *Handbook of Solubility Parameters and Other Cohesion Parameters,* CRC Press, Boca Raton, FL, 1985, p. 64.
17. E. Morel, V. Bellenger, M. Bocquet, and J. Verdu, *J. Mater. Sci.,* **24,** 69 (1989).
18. A. S. Argon and M. I. Bessonov, *Polym. Eng. Sci.,* **17,** 174 (1977).
19. E. F. Oleynik, *Prog. Colloid Polym. Sci.,* **80,** 140 (1989).
20. J. Perez, *Physique et Mécanique des Polymères Amorphes,* Lavoisier, Paris, 1992.
21. J. M. Lefebvre and B. Escaig, *Polymer,* **34,** 518 (1993).